The Space Congress® Proceedings

1987 (24th) Space - The Challenge, The Commitment

Apr 1st, 8:00 AM

University of Florida Lightning Research at The Kennedy Space Center

Martin A. Uman
Professor Department of Electrical Engineering University of Florida, Gainesville 32611

Ewen M. Thomson
Assoc. Professor Department of Electrical Engineering University of Florida, Gainesville 32611

University of Florida Lightning Research at the Kennedy Space Center

Martin A. Uman, Professor
Department of Electrical Engineering
University of Florida, Gainesville 32611

Ewen M. Thomson, Assoc. Professor
Department of Electrical Engineering
University of Florida, Gainesville 32611

ABSTRACT

A variety of basic and applied research programs are being conducted at the Kennedy Space Center. As an example of this research we describe the University of Florida program to characterize the electric and magnetic fields of lightning and the coupling of those fields to utility power lines. Specifically, we consider in detail the measurements of horizontal and vertical electric fields made during the previous three summers at KSC and the simultaneous measurements of the voltages on a 500 m test line made during the past two summers at KSC. Theory to support these measurements is also presented.

INTRODUCTION

The University of Florida (UF) lightning research team has, during the past 15 years, pioneered in the characterization of the vertical electric field and the horizontal magnetic field produced by return strokes in lightning flashes to earth (e.g., Uman, 1985). Recently the UF group has undertaken a study of the horizontal electric field associated with the return stroke and of the coupling of the horizontal field and its associated vertical field to long horizontal wires, notably overhead power lines. In this paper we describe (1) the measurements made at KSC of the properties of the horizontal electric field including its measured and calculated relation to the associated vertical field, and (2) the measurements and supporting theory to describe the coupling of the lightning fields to a 487 m test line specially constructed for this study at KSC.

FIELD MEASUREMENTS

The electric field produced by lightning within about 10 meters of ground is predominantly vertically polarized for frequencies below about 1 MHz. Antennas and electronics for measuring this vertical field in the frequency band from below 1 Hz to over 1 MHz have been described, for example, by Brook and Kitagawa (1960), Fisher and Uman (1972), Krehbiel et al. (1979), and Weidman and Krider (1978, 1982). The antennas employed in these studies were flat circular plates either mounted flush with the earth or elevated. Such antennas have been used to characterize thoroughly the vertical field due to lightning (e.g., Lin et al., 1979, Weidman and Krider, 1978, 1982).

The horizontal component of the lightning field, although smaller than the vertical, is important in that it can be a significant factor in producing voltages on long horizontal conductors such as overhead power lines and buried cables (e.g., Vance, 1978). Since the horizontal field depends both on the vertical field and on the local electrical properties of the ground (e.g., Vance, 1978), which are generally unknown, an in situ measurement of this horizontal component is needed in order that the effects of lightning can be predicted. The horizontal component of the electric field from lightning had not been measured with a wideband system until the UF study beginning in 1984.

We describe first the spherical antenna that we have designed, built, and used to measure simultaneously the two horizontal components and the vertical component of the lightning electric field within a bandwidth of 3 Hz to 4 MHz. More details than are given here can be found in the paper "A remote sensor for the three components of transient electric fields" by Thomson, Medelius, and Uman which has been submitted to the IEEE Transactions on Industrial Electronics. The antenna, a metallic sphere of 45 cm diameter with insulated surface cutouts centered on three orthogonal axes, is supported by an insulating support structure with its center

about 1.5 m, about 3 sphere diameters, above ground, as shown in Fig. 1. At this height, calculations show that the pertubation of the ambient surface charge density on the ground due to the sphere results in an error in measured field magnitude of less than 0.1%. The system block diagram is given in Figure 2. The three electric field signals, one for each orthogonal component, are processed in electronics within the sphere and are sent to the instrumentation rack in the recording station via fiber optics links. A high pass amplifier is necessary to remove a DC bias introduced by each fiber optics receiver. Control signals within the sphere that either change the gain and the lower 3dB frequency of the electric field amplifiers or trigger a calibration signal in the sensor are sent to the sensor via a VHF link.

Electric field components in the vertical and the two perpendicular horizontal directions are sensed by measuring the charge induced on three circular caps which are centered on the three axes of the sphere and electrically isolated from the body of the sphere. For example, the induced charge Q_d on the sensor cap at the bottom of the sphere is the integral of the normal component of the electric flux density over the surface of the cap (e.g., Reitz et al., 1979), which has no net contribution due to field components perpendicular to the z-axis.

The charge Q_d is measured by integrating the conduction current, numerically equal to the displacement current towards and into the cap, that flows from the cap to the body of the sphere through an operational amplifier integrator. The principle of operation of the active integrator is the same as that for circuits used previously to measure the vertical component of the electric field from lightning (e.g., Brook and Kitagawa, 1960).

Measurements of horizontal and vertical electrical fields from lightning return strokes were made at KSC during 1984, 1985, and 1986. The data discussed here were obtained from 42 strokes recorded from lightning at distances from 7 to 43 km during a six minute interval from 1850 to 1856 UT on August 11, 1984. A more complete discussion of these data is found in the paper "Horizontal electric fields from lightning return strokes" by Thomson, Medelius, Uman, Johnson, and Stone which has been submitted to the Journal of Geophysical Research. The electric field signals from the spherical antenna were recorded on Biomation transient waveform recorders and on a Honeywell 101 instrumentation tape recorder.

We independently measured the ground conductivity as a function of depth for a flat area of earth approximately 150 m x 200 m in extent over which the sphere was suspended from measurements obtained using a Bison 2350 B conductivity meter in the standard Wenner four-electrode array. The variation of conductivity with depth was found by considering the earth as being horizontally stratified in four layers. The layer conductivities and depths found were 8.2×10^{-3} mho/m between ground level and 2.2 m, 3.1×10^{-2} mho/m between 2.2 m and 11 m, and 0.2 mho/m between 11 m and 40 m, and 2.5×10^{-3} mho/m below 40 m. These values are consistent with independent sources of information concerning the subterranean structure of the site (Brown et al., 1962).

The alignment of the spherical antenna was particularly important since the horizontal fields measured were typically thirty or more times smaller than the vertical and any tilt would cause a component of the vertical to appear in the horizontal field signals. We oriented the sphere initially with respect to a gravitationally-based vertical axis and then, with reference to the signals from distance lightning, further adjusted the tilt so that the two horizontal field components had essentially similar waveshapes and that no component of the vertical field was obviously evident in the horizontal fields. Any residual effect of tilt was removed by subsequent processing of the data.

Figure 3 shows the three electric field components- vertical (EVERT), northerly (ENORTH), and easterly (EEAST) - from all trigger events in a ground flash at a distance of 7 km, one of the closest recorded. The vertical field in Figure 3(a), from the first trigger event in the flash, contained about 90 μs of impulsive fine structure following the initial peak in a manner characteristic of a first stroke (Uman, 1985). The subsequent stroke whose fields are presented in Figure 3(b) appears to be preceded by a dart-stepped leader even though it followed the first stroke by a time interval of 59 ms, not unduly long for an interstroke interval (Thomson, 1980). The mean step interval in the last 20 μs of the leader was 1.5 μs. The vertical field waveshapes (EVERT in Figures 3(a) and 3(b)) have ramps following the initial peaks in the manner illustrated by Lin et al. (1979) for return strokes at about this distance, and have values of: (i) the ratio of the electric field at 170 μs (extrapolated) to the initial peak (1.7 and 0.9, respectively), (ii) the ramp starting time (20-60 μs and 40 μs), (iii) initial peak field (52 V/m and 101 V/m), and (iv) (extrapolated) field at 170 μs (88 V/m and 91 V/m), that are all in the range obtained by Lin et al. (1979) at Kennedy Space Center for lightning at a distance of 7 km. The horizontal fields

ENORTH and EEAST in Figures 3(a) and 3(b) are largest at times when the vertical field is changing rapidly. In particular, there are no discernible horizontal fields (within the resolution defined by the noise level of these records) associated with the ramp field changes. The two horizontal field waveshapes are similar within 30 μs of the initial peak, but there are subtle differences at later times. Even though the overall change in the vertical field is roughly the same magnitude from the start of the return stroke (t = 50 μs) until the end of the record (t = 200 μs), 150 μs later, the peak vertical field for the subsequent stroke is roughly twice the size of that for the first stroke, and the horizontal peak fields for the subsequent stroke are about four times the size of those for the first stroke.

We now characterize the horizontal electric field waveshapes associated with the initial peak in the vertical field for all 42 strokes. These waveshapes are influenced by the ground conditions at the measurement site as well as by the characteristics of the source lightning and its distance. For all horizontal pulses analyzed, the horizontal field peak preceded the associated vertical field peak. The distribution of the peak horizontal to vertical field ratio is summarized in the histogram of Figure 4. The mean value of the ratio was 3.0×10^{-2} and the standard deviation was 0.7×10^{-2}. The horizontal field pulses were not appreciably skewed: the mean half-value-to-peak risetime was 0.32 μs while the mean peak-to-half-value falltime was 0.30 μs.

We found the theoretical horizontal field magnitude from the vertical electric field by using the time domain approach of Master (1982) which is based on the wavetilt frequency domain transfer function valid for vertically polarized fields at grazing incidence to a uniform earth (e.g., Vance, 1978)

$$E_H(\omega) = \frac{1}{[\varepsilon/\varepsilon_0 + \sigma/j\omega\varepsilon_0]^{1/2}} \; E_V(\omega)$$

where $E_H(\omega)$ and $E_V(\omega)$ are the fourier transforms of the horizontal and vertical fields, respectively, σ is the conductivity and ε the permittivity of the ground, ε_0 is the permittivity of free space, and ω is the angular frequency. We assumed that the conductivity of the earth was 8×10^{-3} mho/m, the value found for the top layer of ground (between the surface and a depth of 2.2 m). For the range of observed conductivities and a ground permittivity of $40\varepsilon_0$ or less, the waveshape of the computed horizontal field was insensitive to either the magnitude of the ground conductivity or the permittivity while the magnitude of the computed horizontal field varied inversely as the square root of the conductivity. This is the case because the second term under the square root in the wave tilt expression dominates the first for frequencies below the upper frequency limit of the experiment, about 5 MHz.

The measured and calculated horizontal electric fields for the two strokes in Figure 3 are presented in Figure 5 for comparison. A common feature in all fields is the fairly good agreement for the field peaks and consistently smaller measured field for the more slowly varying parts of the waveforms.

LINE VOLTAGES

The modeling of voltages induced on horizontal wires by external electric and magnetic fields is an important area of modern research in electromagnetics. The particular case of interest here is the study of lightning induced voltages on distribution power lines. Several models have been devised to allow calculation of the lightning induced voltage on power lines (e.g., Agrawal et al., 1980; Kami and Sato, 1985), but none has been successfully compared to experiment (e.g., Koga et al., 1981; Master and Uman, 1984). The approximations made in the theoretical models are discussed by Agrawal et al. (1980) and Kami and Sato (1985). In the present study, the time domain transmission line model developed by Agrawal et al. (1980) has been adopted to calculate the induced voltages due to distant lightning.

The equivalent circuit model of Agrawal et al. (1980) for the case of a single-wire above a finite conducting ground as shown in Fig. 6 can be expressed as

$$\frac{\partial}{\partial x} V^s(x) + RI(x) + \frac{\partial}{\partial t} I(x) = E^i_x(x)$$

$$\frac{\partial}{\partial x} I(x) + C \frac{\partial}{\partial t} V^s(x) = 0$$

and $$V^T(x) = V^s(x) - \int_0^b E^i_z(x,z)\, dz$$

where $V^s(x)$, $V^T(x)$, $E^i_x(x)$ and $E^i_z(x,z)$ are the scattered and total voltages, and the horizontal and vertical electric fields along the line, respectively. In the equivalent circuit, the resistance per unit length R is effectively Rg, the resistance of the earth per unit length, which is approximately $\mathrm{Re}(Zg) = \frac{1}{4}\pi b\sigma\delta$ when $\delta \ll 2b$, $\sigma \gg \omega\varepsilon$ and $\mathrm{Re}(Zg) = \omega\mu/\delta$ when $\delta \gg 2b$ (Vance, 1978), where b is the height of the cable above ground, δ is the skin depth, and Zg is the

impedance of ground. In this study, the effective one layer σ near the test line (a different site at KSC, the rocket triggering site, from that at which the data given in the previous section were acquired) was determined from horizontal and vertical electric field measurements to be 1.6×10^{-2} mhos/meter, a relatively high conductivity. Rg is calculated, for simplicity, only for a frequency of 1 MHz and hence is treated as a constant. The inductance L and capacitance C per unit length of the line were calculated by a separate computer program for the generalized case of the 3-phase line used. In order to solve the generalized variation of the nonhomogeneous differential equations given above numerically, a finite difference scheme was used.

To illustrate the validity of this transmission line algorithm, a half-sinewave pulse vertical electric field $E_v(t)$ and its corresponding horizontal electric field $E_h(t)$ due to the finite conducting ground calculated by the wavetilt formula (see previous section) as shown in Fig. 7 were used as the forcing terms to excite a 487 meter long 3-phase line. In the first case, E_v only comes in from the left-end and both ends are open-circuited. The induced voltages computed at the left-end, middle, and right-end points of the line are shown in Fig. 8-a. The voltage is simply the opposite polarity of E_v times the line height with the necessary time delay at the measuring point. The existence of a vertical electric field causes the charges in the conductor to separate in a direction perpendicular to the line, and thus no net current flows along the line. When we add E_h to the driving force to compute the induced voltage for the same system configuration, the result is shown in Fig. 8-b. The induced voltage within the first microsecond is mainly due to E_v since the voltage due to E_h becomes appreciable only after E_h has been applied to an appreciable length of the line. Later, the voltage component due to E_h become significant. Note that in the third microsecond, the signals due to the effects of E_h reflected from the right-end arrive at the left-end. The voltages continue to oscillate with a period of about 3 μsec with a damped amplitude due to the finite ground conductivity. The initial peak voltage at the middle and right-end points of the line are due to the combined effect of E_v and E_h. At the middle point, the oscillating frequency of the induced voltage is twice that at the two ends since it only takes half the time for the signal to travel to the ends and reflect back to the middle. A similar discussion applies to the case in which one end of the line is terminated in the line's characteristic impedance, but in that case only one reflection from the open end occurs since the reflected signal is absorbed by Z_0 when it arrives at the left-end. The induced voltages for this case are shown in Fig. 9a,b.

The 487-meter long power line was instrumented for induced voltage measurement at the rocket triggering site at KSC and such measurements were made during 1985 and 1986. Simultaneously, the spherical antenna was used to measure E_v and E_h, two flat plate antennas were used as redundant E_v sensors, and the two horizontal components of the magnetic field were measured with loop antennas. Voltage signals from the power line were transmitted through fiber optical cables to waveform recorders. At each end of the power line, we could also select a termination of 500 Ω, 600 Ω, or 1 MΩ.

For the data presented here, the induced voltage and two perpendicular components of the horizontal magnetic field B were measured simultaneously. For lightning at the range studied, E_v and B have identical waveshapes for tens of microseconds since for that time both are essentially radiation fields, and hence B can be measured in place of E_v. An added advantage of measuring the magnetic fields is the determination of the direction to the lightning.

To analyze and compare the experimental results with the theoretical prediction, the measured induced voltage data and the E_v data were transferred to a MASSCOMP MC-5500 computer system. First, E_h was computed using the wavetilt formula with the previously determined value for ground conductivity. Then, induced voltages were calculated based on the line parameters and the input E_v and E_h driving functions using the transmission line coupling code. Forty-three return-strokes were studied. They were divided into three groups depending on line terminations: both ends open, left-end 500 Ω and right-end open, and left-end 600 Ω and right-end open. Except for 5 abnormal events (4 with both ends open, 1 with left-end 600 Ω) with a difference ranging from -58.2% to 132.4%, the percent difference between measurement and theoretical prediction are all less than 35%. Typical waveshapes for both ends of the line open and each end terminated are shown in Fig. 10, 11, and 12, respectively.

The agreement between theory using measured fields and experimental voltage waveshapes is reasonable considering the various sources of error such as the effect of a ground conductivity that potentially changed with position along the line as the line comes closer to a body of salt water and trees on one side of the power line.

ACKNOWLEDGEMENT

This research was supported in part by NSF grant ATM8217036, DOE contract 19X-8950C via Martin Marietta Energy Systems, Inc., Oak Ridge National Laboratory, and NASA contract NAS10-11020.

REFERENCES

Agrawal, A.K., H.J. Price, and S.H. Gurbaxani, "Transient response of multi-conductor transmission lines excited by a nonuniform electromagnetic field," IEEE Trans. Electromagn. Compat. Vol. EMC-22, No. 2, pp 119-129, 1980.

Brook, M., and N. Kitagawa, Electric-field changes and the design of lightning-flash counters, J. Geophys. Res., 65, 1927-1931, 1960.

Brown, D.W., W.E. Keanel, J.W. Crooks, and J.B. Foster, Water Resources of Brevard County, Florida Geological Survey Report of Investigations No. 28, 1962.

Fisher, R.J., and Uman, M.A., Measured electric field risetimes for first and subsequent lightning return strokes, J. Geophys. Res., 77, 399-406, 1972.

Kami, Y. and R. Sato, "Circuit-concept approach to externally excited transmission lines," IEEE Trans. Electromagn. Compat. Vol. EMC-27, No. 4, pp 177-190, 1985.

Koga, H., T. Motonitsu, and M. Taguchi, "Lightning surge waves induced in transmission lines," Rev. of the Elec. Comm. Lab., Vol. 29, No. 7-8, pp 797-809, 1981.

Krehbiel, P.R., Brook, M., and McCrory, R., An analysis of the charge structure of lightning discharges to the ground, J. Geophys. Res., 84, 2432-2456, 1979.

Lin, Y.T., M.A. Uman, J.A. Tiller, R.D. Brantley, E.P. Krider, and C.D. Weidman, Characterization of lightning return stroke electric and magnetic fields from simultaneous two-station measurements, J. Geophys. Res., 84, 6307-6314, 1979.

Master, M.J., "Lightning induced voltages on power lines: theory and experiment," Ph.D. Dissertation, University of Florida, Gainesville, Florida, 1982.

Master, M.J., and M.A. Uman, "Lightning induced voltages on power lines: theory," IEEE Trans. Power Appra. Syst., Vol. PAS-103, No. 9, pp 2503-2518, 1984.

Reitz, R.J., F.J. Milford, and R.W. Christy, "Foundations of Electromagnetic Theory," Third Edition, Addison-Wesley, 1979.

Thomson, E.M., The dependence of lightning return stroke characteristics on latitude, J. Geophys. Res., 85, 1050-1056, 1980.

Uman, M.A., Lightning return stroke electric and magnetic fields, J. Geophys. Res., 90, 6121-6130, 1985.

Vance, E.F., "Coupling to shielded cables," New York, John Wiley & Sons, 1977.

Vance, E.F., Coupling to shielded cables, John Wiley and Sons, new York, 1978.

Weidman, C.D., and E.P. Krider, The fine structure of lightning return stroke wave forms, J. Geophys. Res., 83, 6239-6247, 1978.

Weidman, C.D., and E.P. Krider, Correction to the 'fine structure of lightning return stroke waveforms', J. Geophys. Res.,87, 7351, 1982.

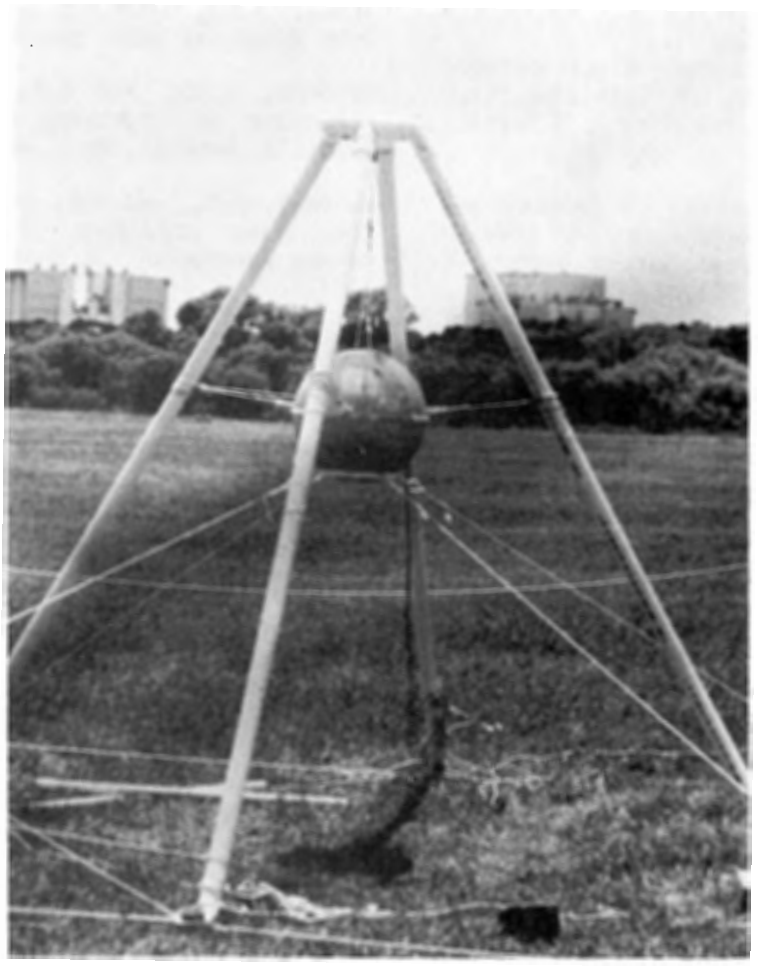

Fig. 1 Spherical electric field sensor and support

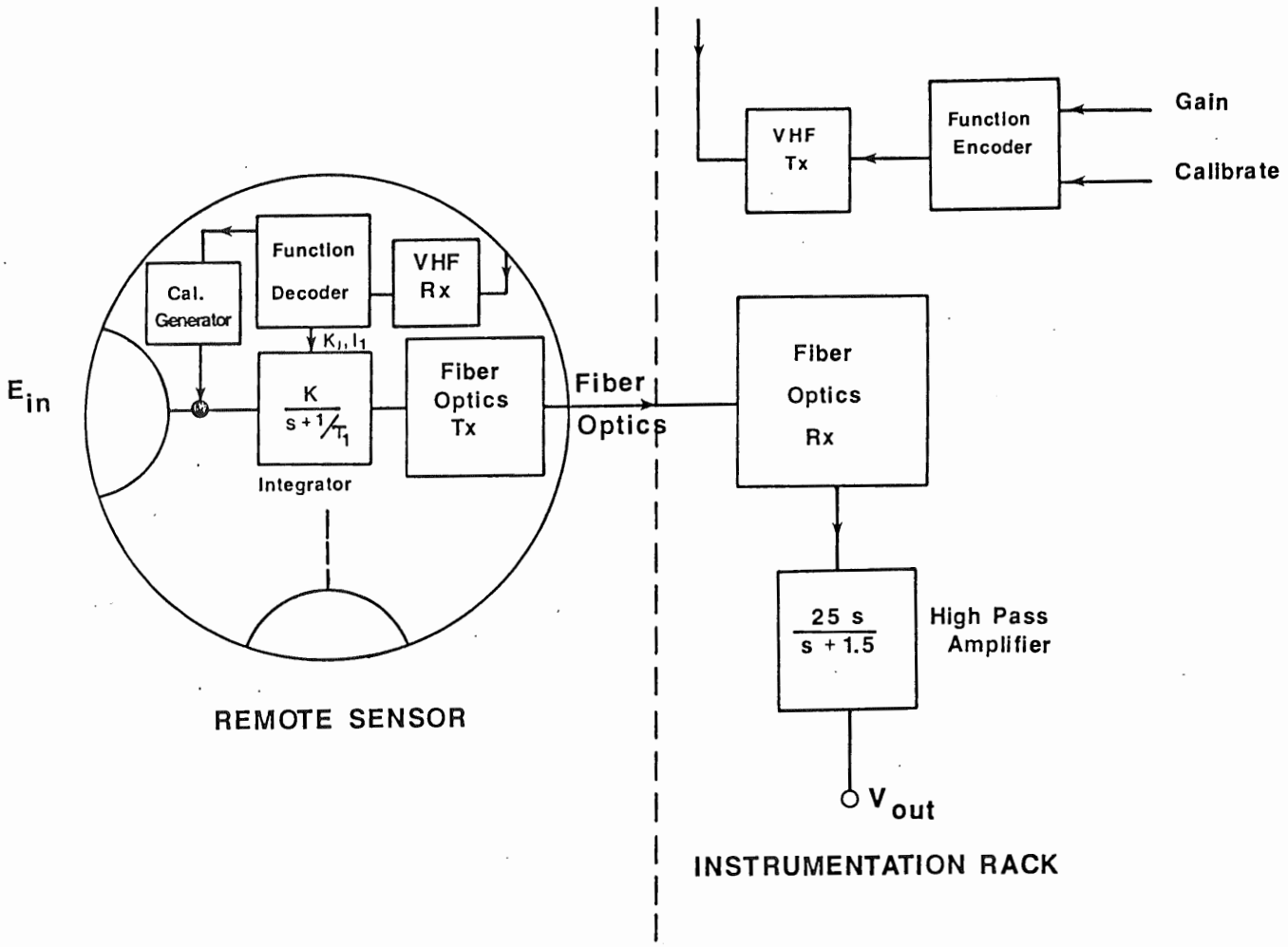

Fig. 2 Block diagram for spherical electric field sensor

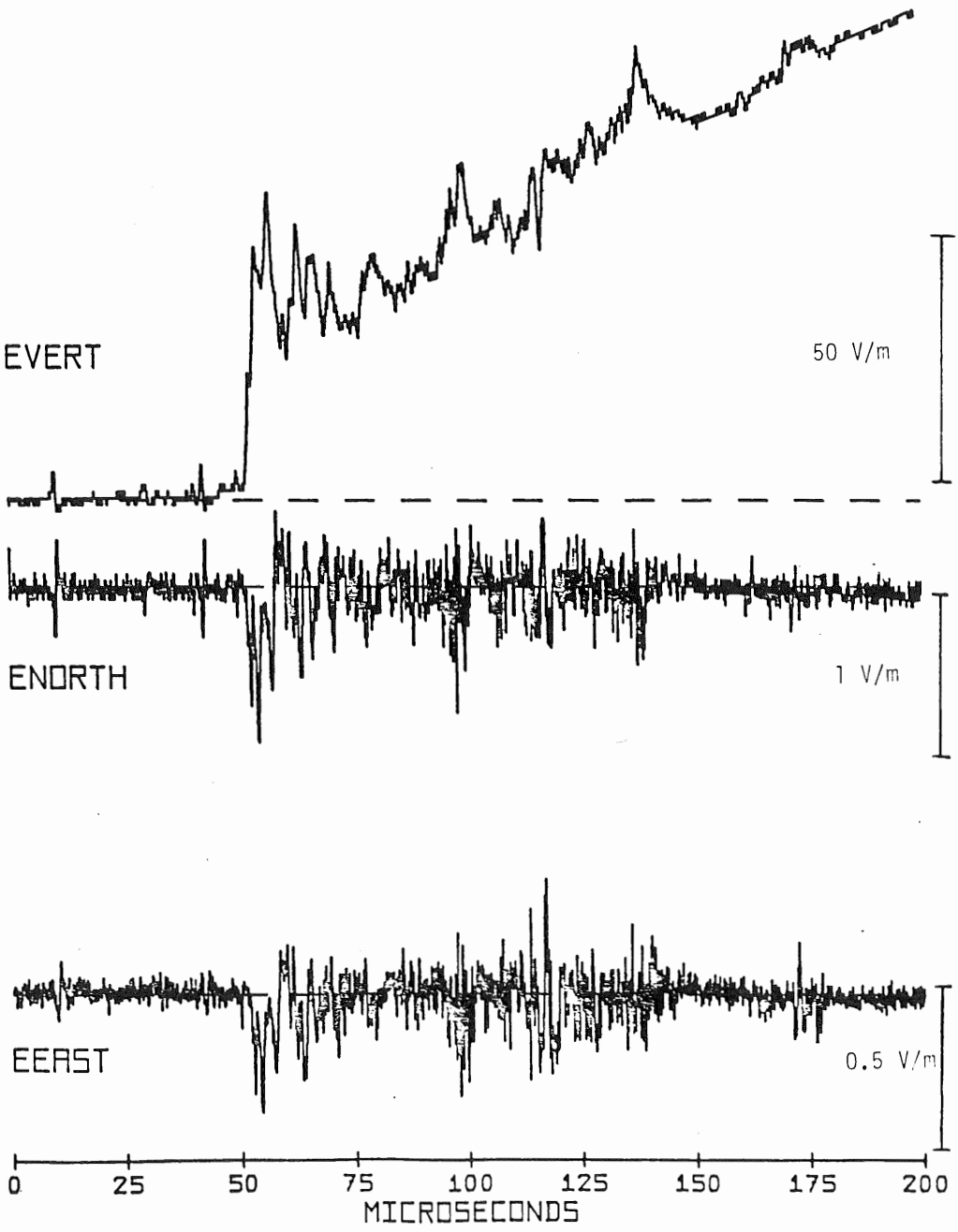

Fig. 3(a) Vertical (EVERT) northerly (ENORTH) and easterly (EEAST) components of electric field from return strokes on July 11, 1984 at time (hour/minute/second) 18/52/43.291. Horizontal and vertical fields are on different scales.

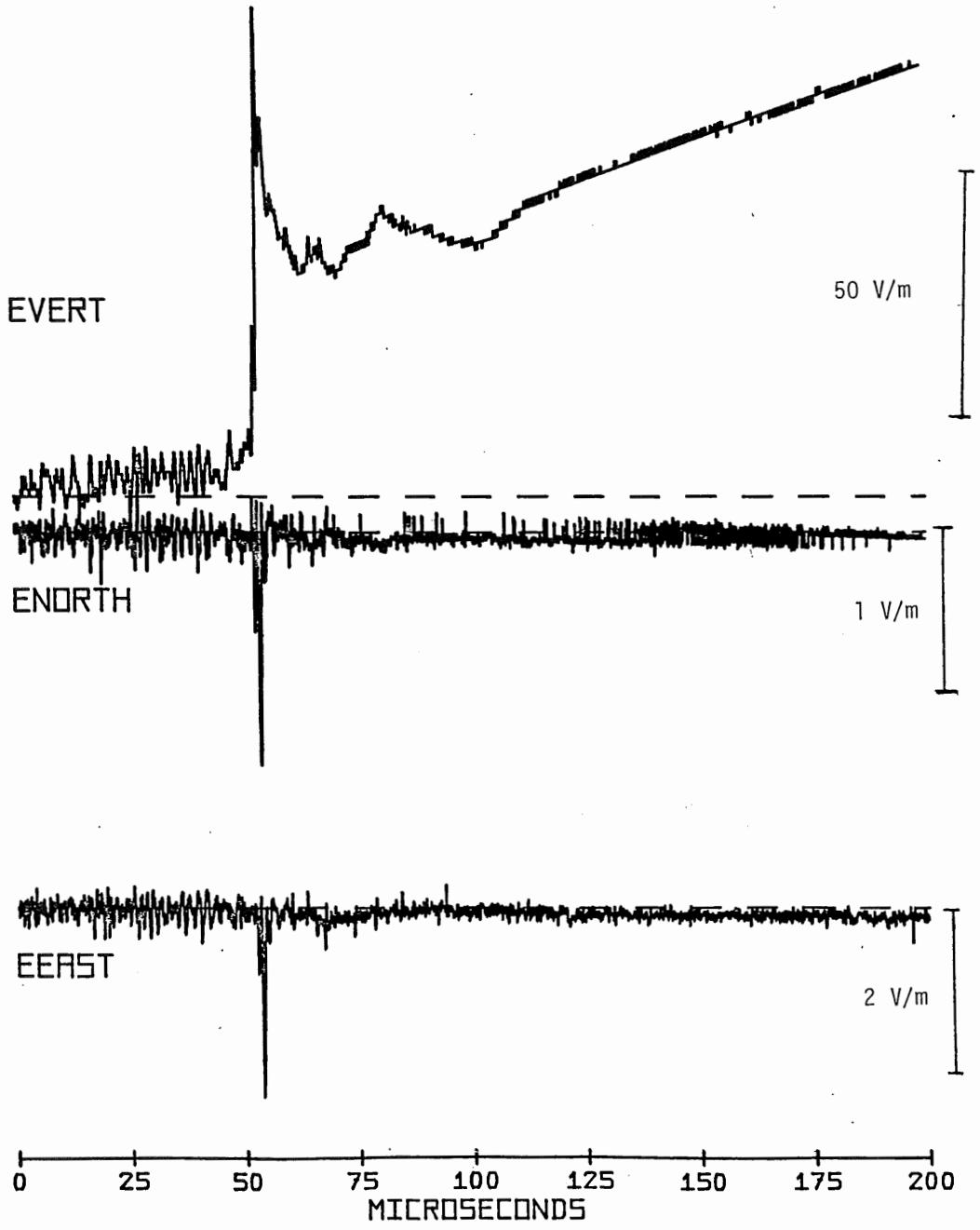

Fig. 3(b) Vertical (EVERT) northerly (ENORTH) and easterly (EEAST) components of electric field from return strokes on July 11, 1984 at time (hour/minute/second) 18/52/43.340. Horizontal and vertical fields are on different scales.

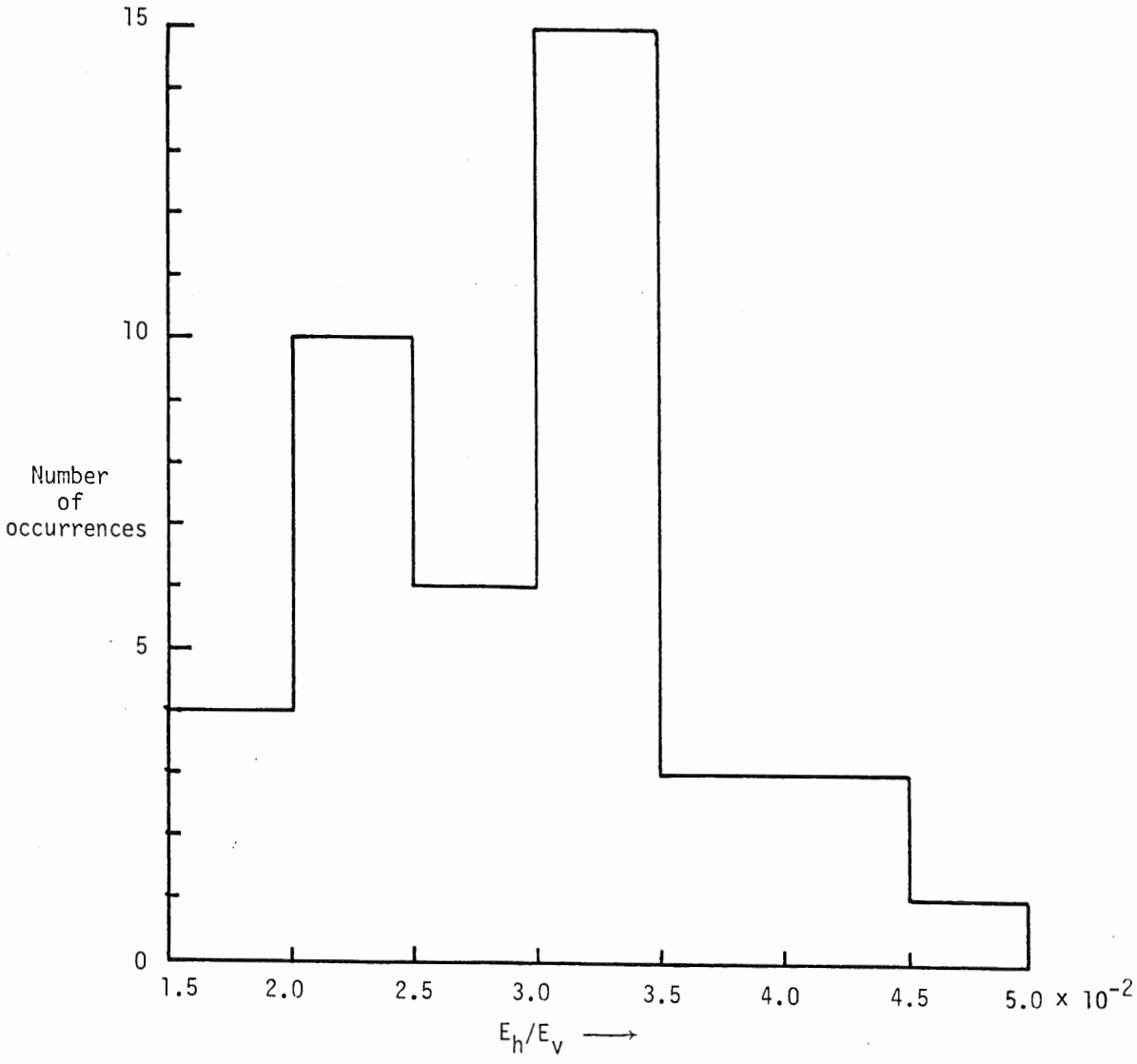

Fig. 4 Histogram of the ratio of horizontal to vertical electric field peaks for 42 strokes occurring on July 11, 1984

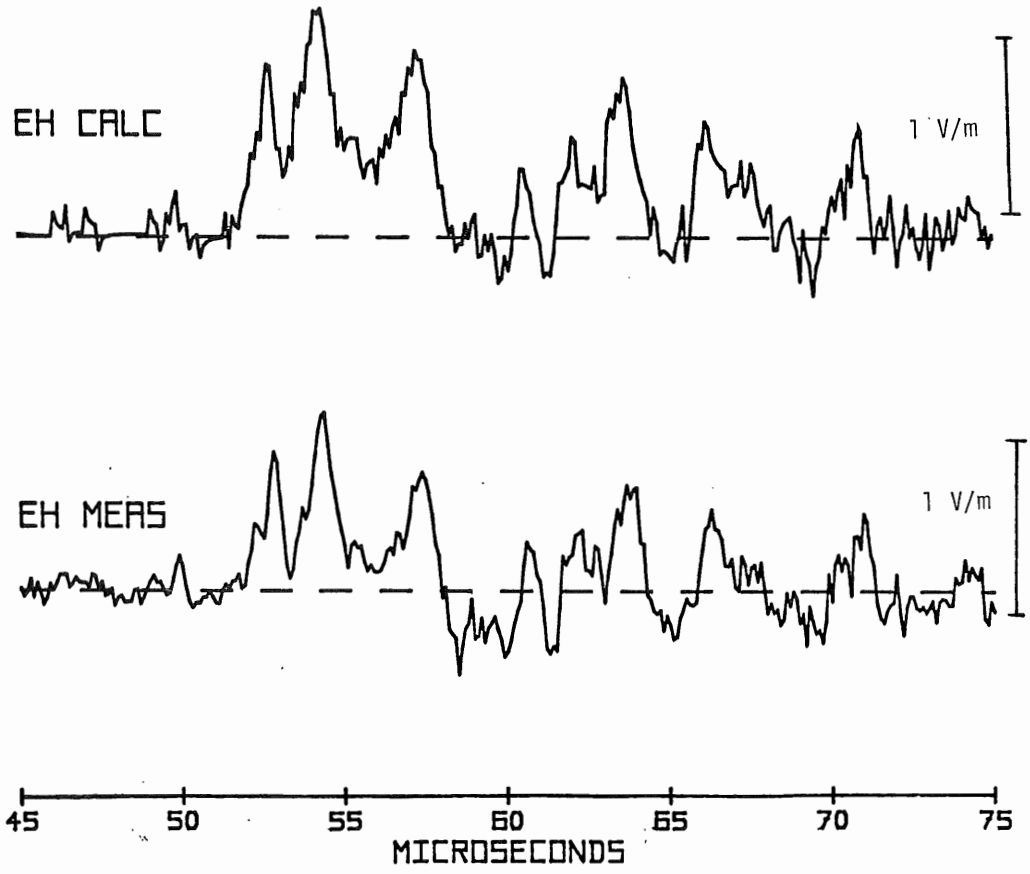

Fig. 5(a) Measured (EH-RMS) (top trace) and calculated (EH-Calc) (bottom trace) horizontal electric fields for return strokes on July 11, 1984 at time (hour/minute/second) 18/52/43.281.

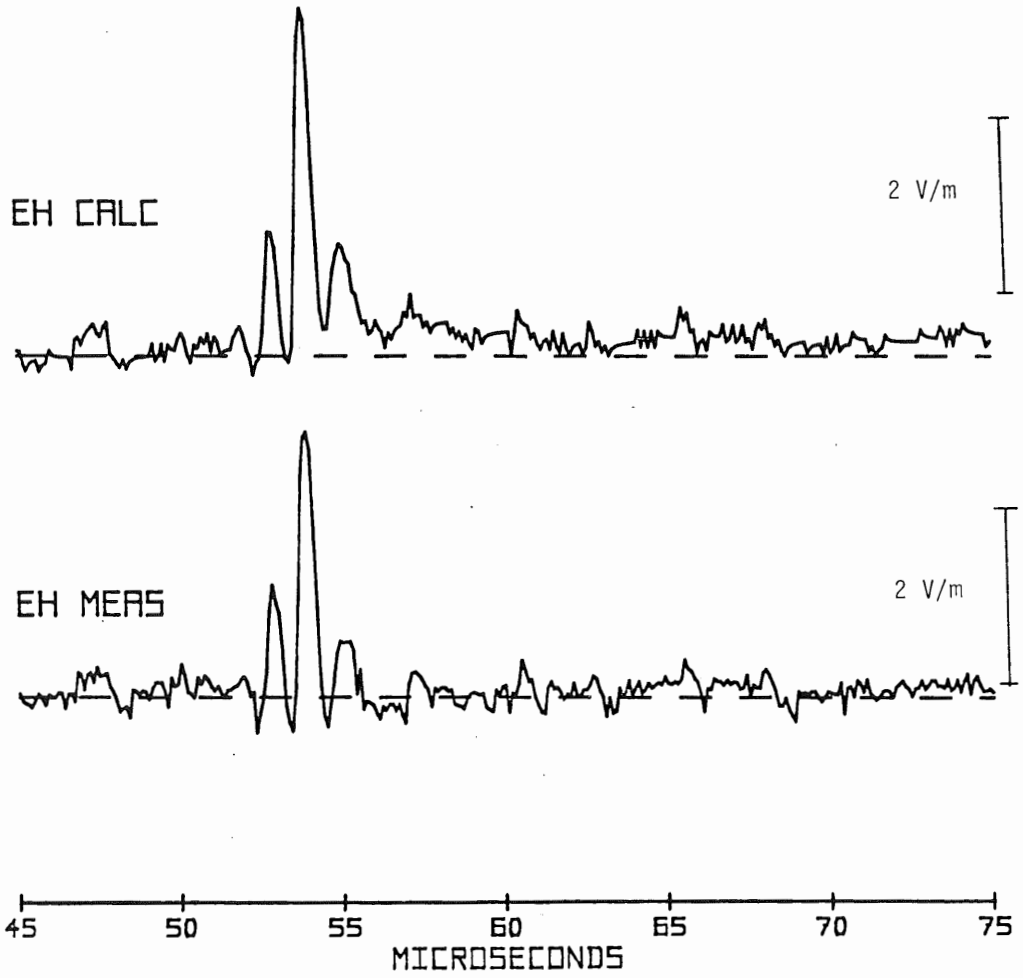

Fig. 5(b) Measured (EH-RMS) (top trace) and calculated (EH-Calc) (bottom trace) horizontal electric fields for return strokes on July 11, 1984 at time (hour/minute/second) 18/52/43.340.

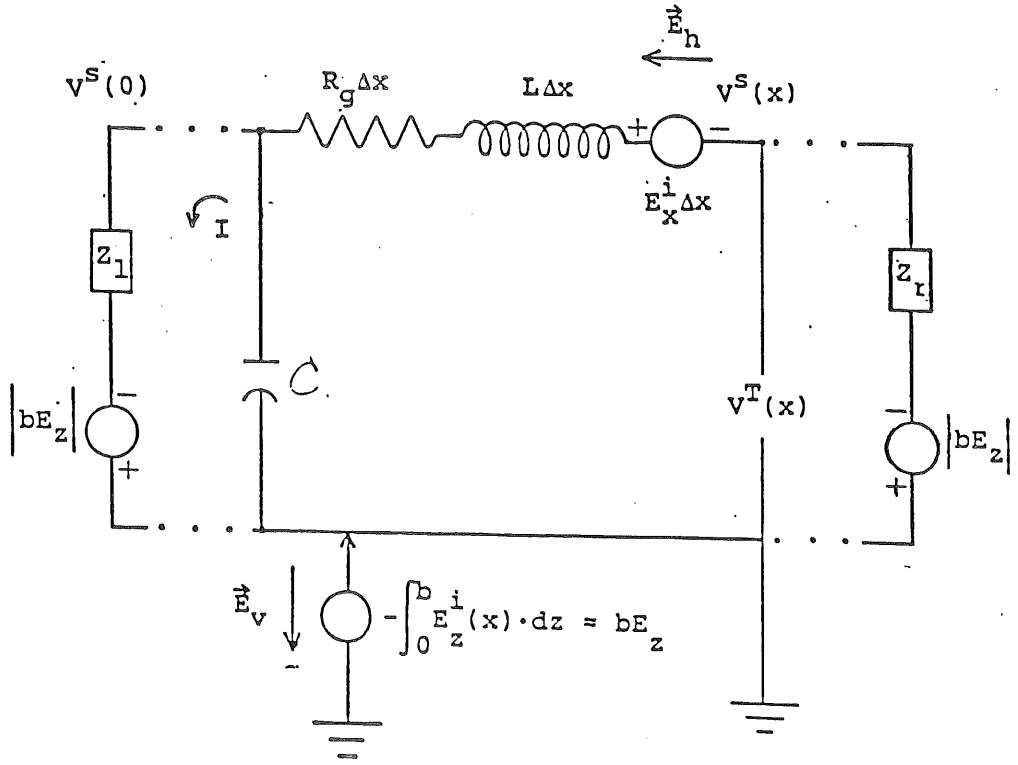

Fig. 6 Equivalent circuit of the time-domain transmission line model for one-wire above ground.

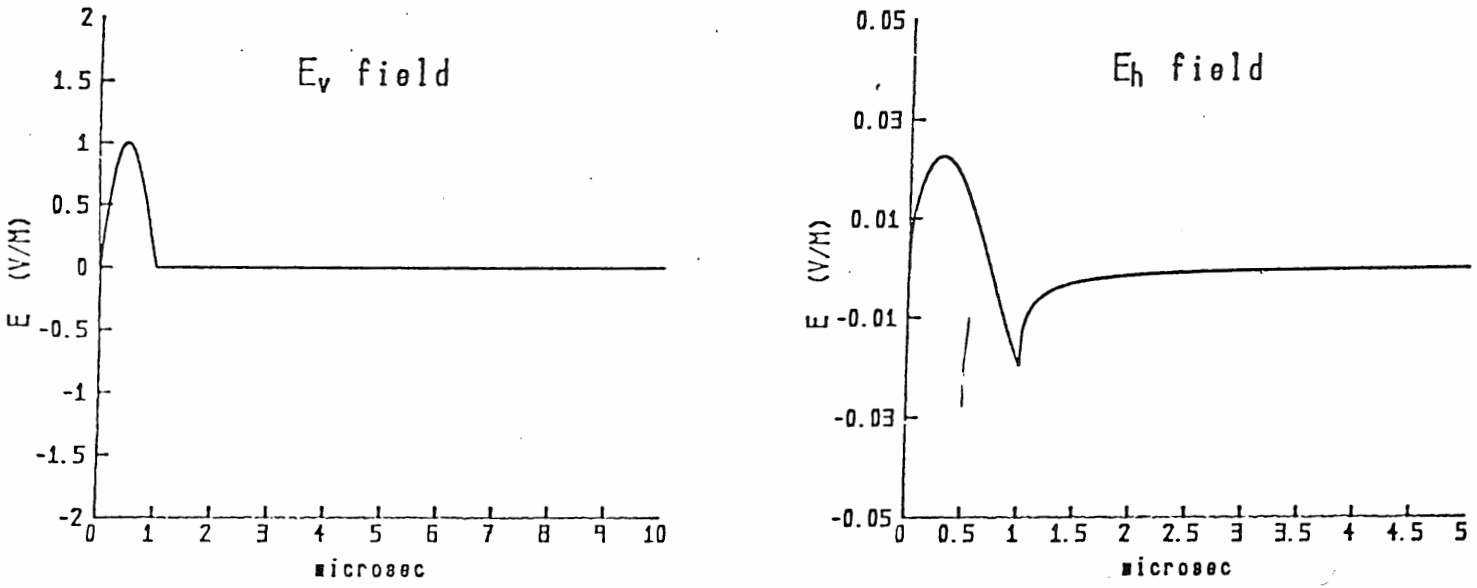

Fig. 7 Assumed E_v field on left and E_h field on right, calculated using the wavetilt formula with $\sigma = 1.62 \times 10^{-2}$ mhos/m, the approximate ground conductivity at the test site.

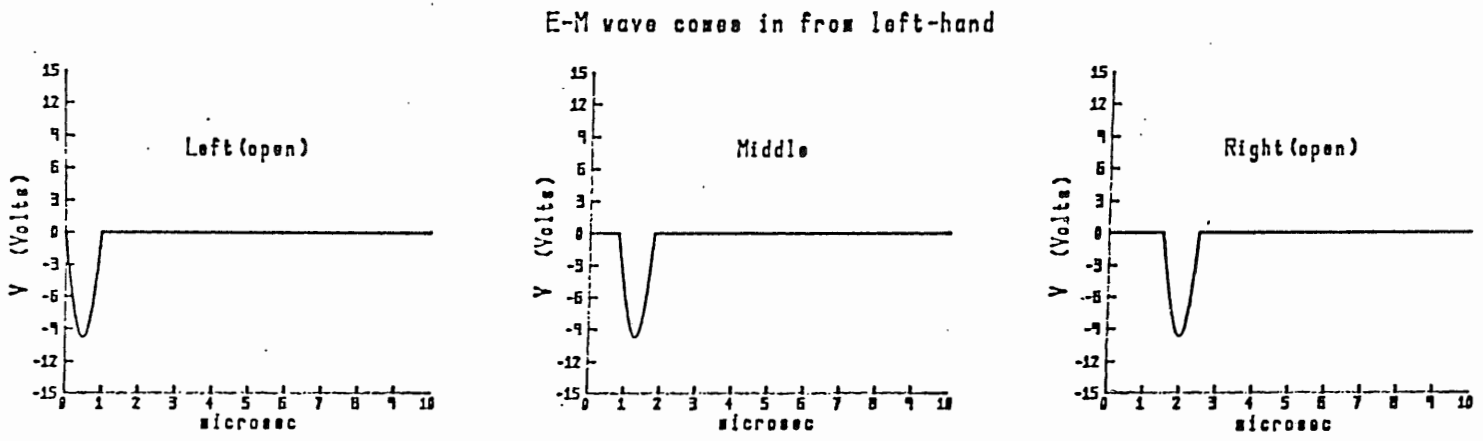

Fig. 8(a) Voltage on the left, middle and right end of a 487 meter line, open-circuited at each end when only the E_v field from Fig. 7 propagates in from the left.

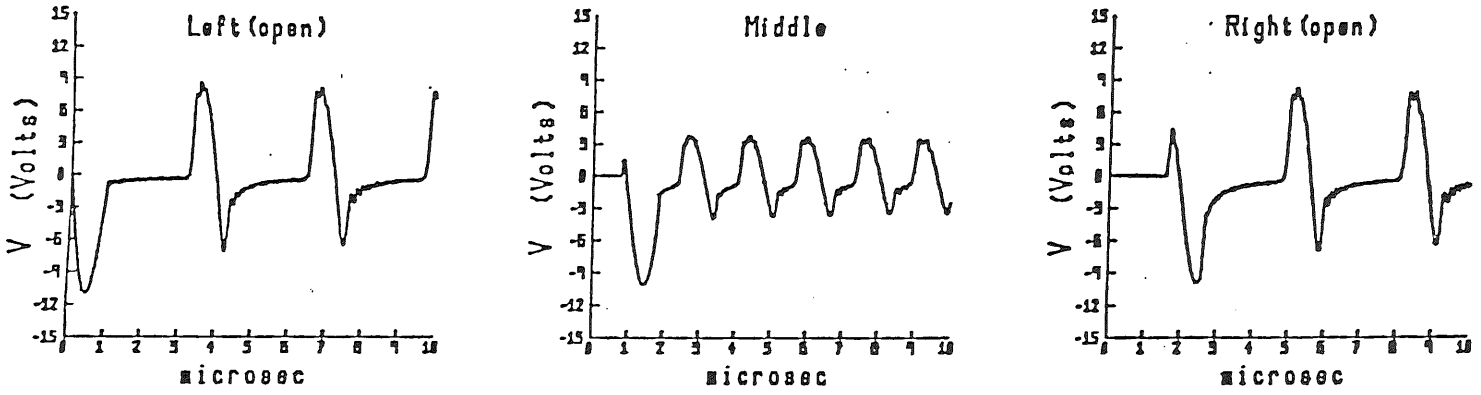

Fig. 8(b) Voltage on the left, middle and right end of a 487 meter line, open-circuited at each end when both the E_v and E_h fields from Fig. 7 propagate in from the left.

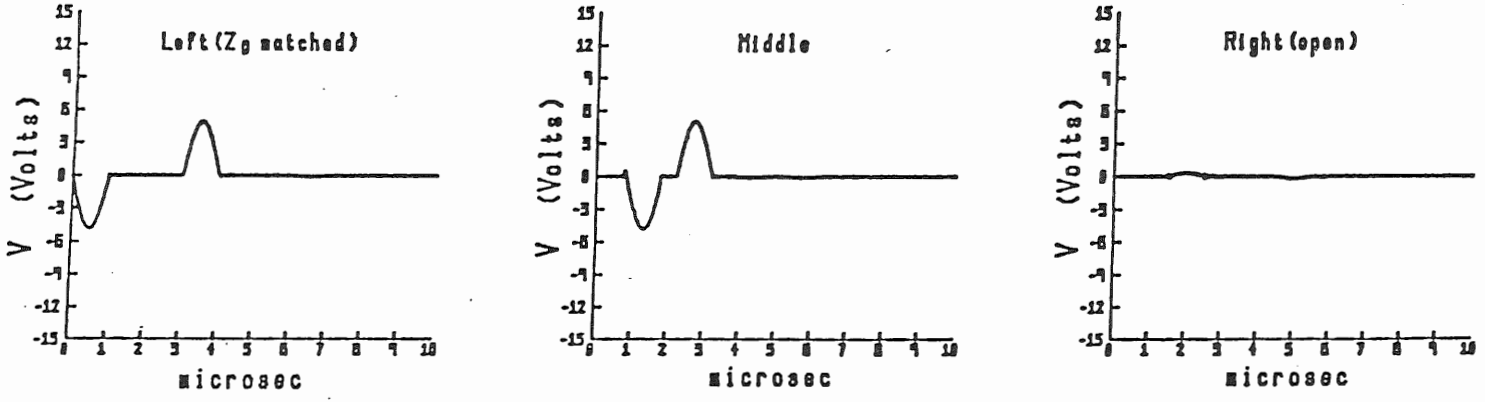

Fig. 9(a) Voltage on the left, middle, and right end of a 487 meter line, open-circuited at right-end, left end terminated in the line's characteristic impedance when only the E_v field from Fig. 7 propagates in from the left.

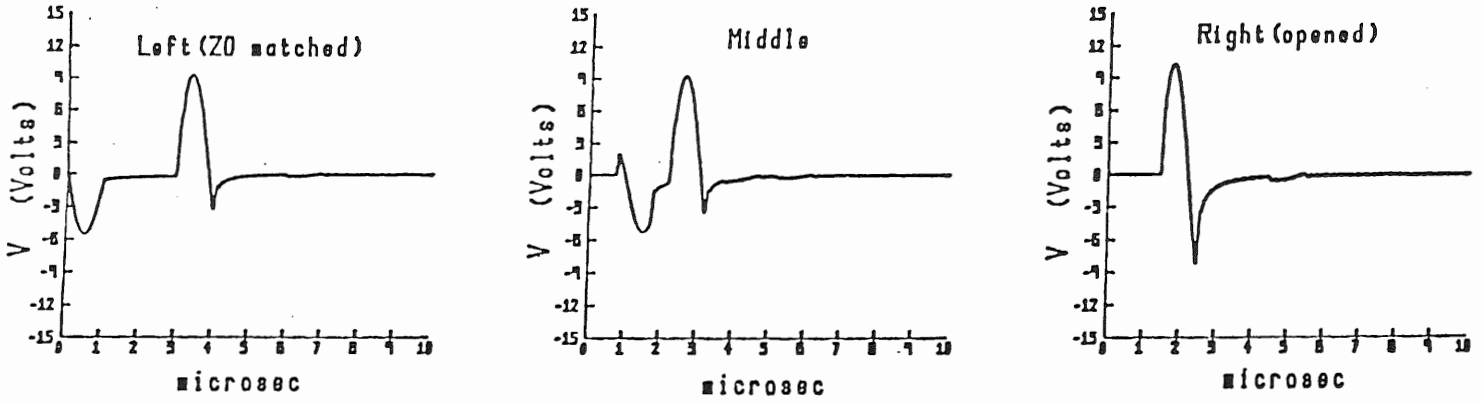

Fig. 9(b) Voltage on the left, middle, and right end of a 487 meter line, open-circuited at right-end, left end terminated in the line's characteristic impedance when both E_v and E_h fields from Fig. 7 propagate in from the left.

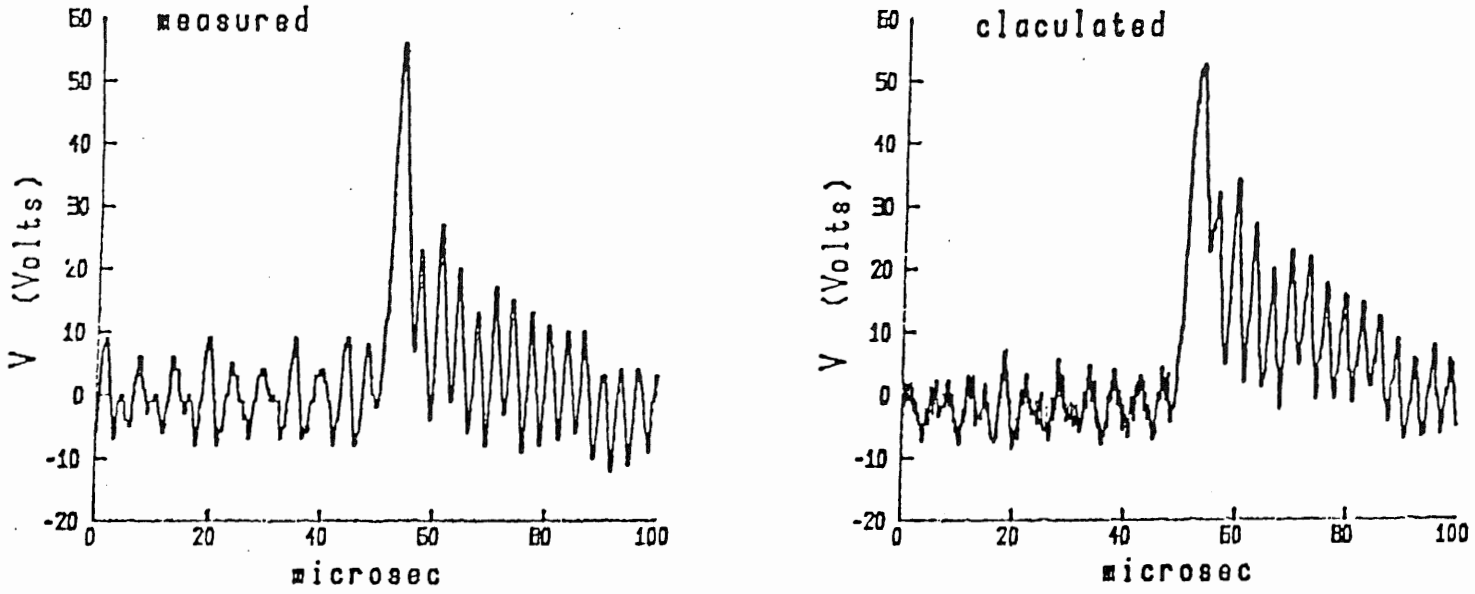

Fig. 10 Waveshape comparison for both ends open-circuited case, incident angle -6.2^0, that is, almost along the line coming over the measurement end first.

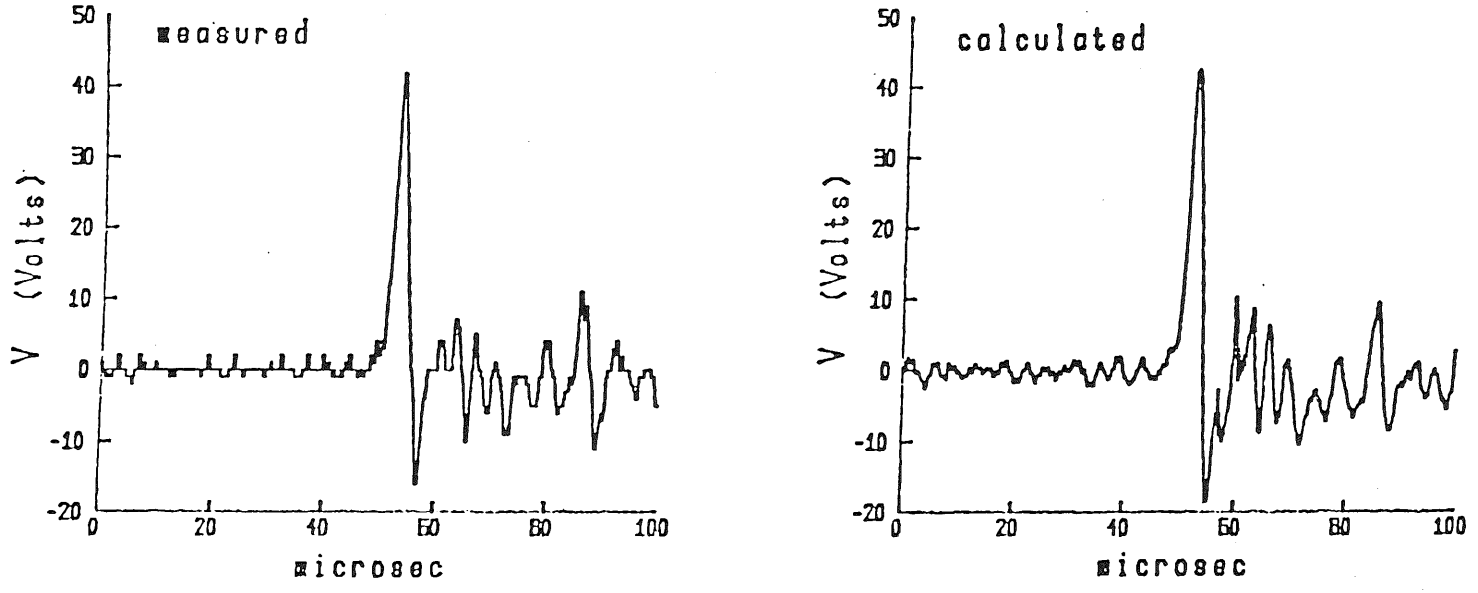

Fig. 11 Waveshape comparison for the left-end 500 Ω terminated incident angle 43.4^0.

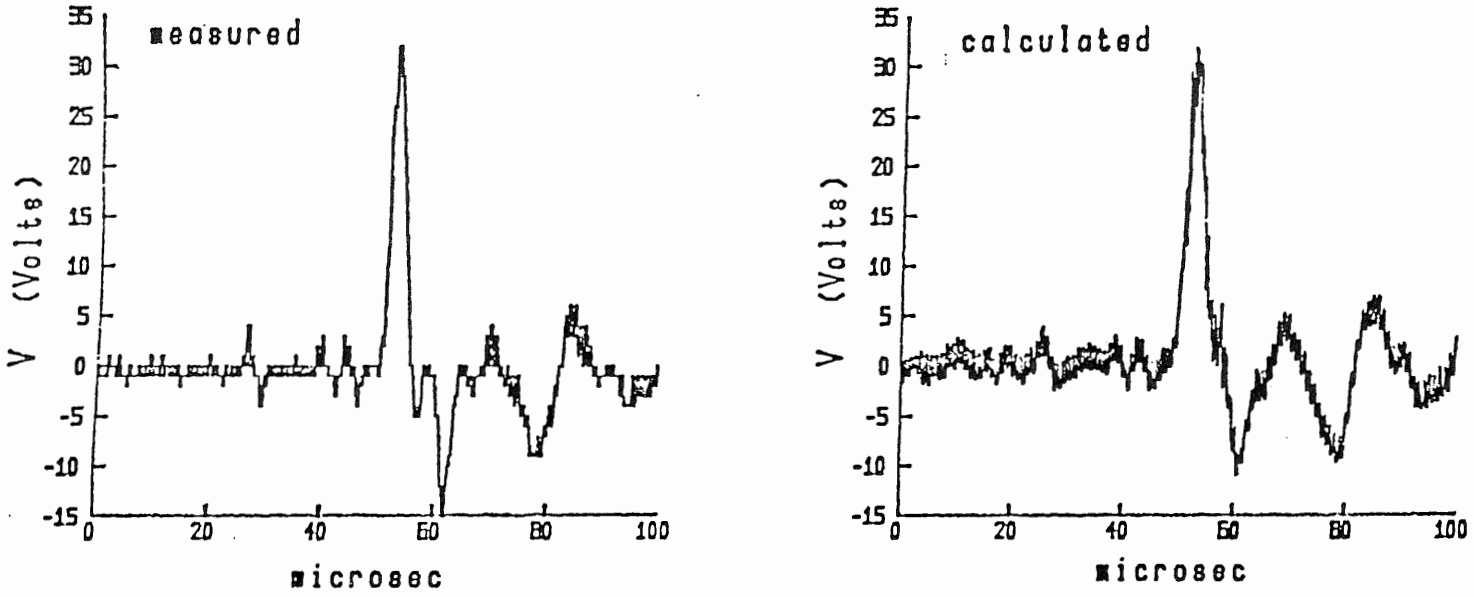

Fig. 12 Waveshape comparison for the right end 600 Ω terminated incident angle -75.6^0, or nearly perpendicular to the line.